JOURNAL OF THE KOREAN INSTITUTE OF ELECTROMAGNETIC ENGINEERING AND SCIENCE, VOL. 11, NO. 4, DEC. 2011 JKIEES 2011-11-4-03

http://dx.doi.org/10.5515/JKIEES.2011.11.4.250

Using Subspace Pursuit Algorithm to Improve Performance of the Distributed Compressive Wide-Band Spectrum Sensing

Le Thanh Tan · Hyung-Yun Kong

Abstract

This paper applies a compressed algorithm to improve the spectrum sensing performance of cognitive radio technology. At the fusion center, the recovery error in the analog to information converter (AIC) when reconstructing the transmit signal from the received time-discrete signal causes degradation of the detection performance. Therefore, we propose a subspace pursuit (SP) algorithm to reduce the recovery error and thereby enhance the detection performance. In this study, we employ a wide-band, low SNR, distributed compressed sensing regime to analyze and evaluate the proposed approach. Simulations are provided to demonstrate the performance of the proposed algorithm.

Key words: Wide-Band Spectrum Sensing, Subspace Pursuit Algorithm, Cognitive Radio, Compressed Sensing, Power Spectrum Density Estimate.

Ⅰ. Introduction

Fueled by the dramatically increasing demand for high quality of services, numerous novel wireless technologies have been invented and are leading to a crowding of spectrum allocation. This, in turn, raises the critical problem that insufficient spectrum space is available for new kinds of application. However, most of the licensed bands are sporadically located and under-utilized, rather than in actual shortage. In fact, less than 5 % of the total licensed spectrum may be in use [1]. The Federal Communications Commission (FCC) has therefore proposed the idea of an open licensed frequency band, which unlicensed users would be allowed to occupy opportunistically. In addition, the IEEE 802.22 workgroup has built the standards of WRAN based on cognitive radio (CR) techniques [2]. CR is now considered as the most competitive candidate for a secondary system that could co-exist with the primary one.

Based on the ability to provide high data rates and high quality of services, wide-band applications are receiving increasingly more attention recently. However, wide-band applications in CR encounter considerable challenges in spectrum sensing. On the one hand, wide-band sensing applications usually employ a large number of RF devices to deal with the wide frequency range. On the other hand, a trade-off exists between high-speed processing units and detection performance due to the sensing time constraints and insufficient samples.

In order to provide a reliable but low complexity model, many studies have exploited a compressed sensing (CS) framework for wide-band sensing. Initially, the CS theory, which was innovated by Donoho [3], allowed a highly sparse signal to be reconstructed from a small number of measurements. In other words, this method is able to compress the sparse signal at the sub-Nyquist rate during sampling in the first stage. The reconstruction stage requires state-of-the-art algorithms to solve the convex optimization problem; for example, the basic pursuit (BP) or orthogonal matching pursuit (OMP) [3], [4]. Zhi et al. [5] next presented a single wide-band CR model that uses CS based spectrum sensing schemes; however, the input signal was still sampled by an analog-to-digital convertor (ADC) operating at a Nyquist rate. The authors in [6] improved compressive wide-band spectrum sensing (CWSS) systems for single CR by employing an analog-to-information converter (AIC) [7]~[9], which operates at a sub-Nyquist rate due to direct application of CS to the analog signal. This group [10] further extended their early work to multiple CRs in order to design a distributed CWSS (DCWSS) based on [11]. These studies simply applied wide-band spectrum sensing to CS; hence, improvement of the model is still required for greater robustness of the performance of spectrum sensing.

In this work, we adopt CWSS and DCWSS schemes for single and multiple CRs, respectively. In addition, we propose the use of the subspace pursuit (SP) method [12] in the reconstruction stage. The novel SP method provides the robustness to cope with inaccurate measure-

Manuscript received July 19, 2011 ; revised October 25, 2011. (ID No. 20110719-022J)

School of Electrical Engineering, University of Ulsan, Ulsan, Korea.

Corresponding Author : Hyung-Yun Kong (e-mail : hkong@mail.ulsan.ac.kr)

ment (due to noisy environment) as well as efficiency and low complexity, owing to its restricted isometry property (RIP) [13]. In an undesirable condition of low SNR licensed signals, we also propose a DCWSS based SP (DCWSSSP) method that jointly reconstructs the sparse signal from multi-CR received signals. Finally, we compare the performance of the DCWSSSP algorithm with those of the schemes using compressive sampling matching pursuit (Cosamp) [12] and OMP [6], [10] to illustrate the accuracy of the proposed method.

The rest of this paper is organized as follows: section Ⅱ presents the relevant concepts and terminology of the CS reconstruction, while a compressive spectrum-sensing scheme for single CR is presented in Section Ⅲ. An extension to the collaborative compressed spectrum sensing for multiple CR is shown in Section Ⅳ, while Section V demonstrates the corroborating simulation results to illustrate the effectiveness of the novel approach in detecting the spectrum holes. Finally, concluding remarks are given in Section Ⅳ.

Ⅱ. Preliminaries

2-1 Signal Model

We assume that the frequency range of the signal consists of max I channels with equal bandwidth. The spectrum-sensing model presented here includes a fusion center that collects data from J CR nodes. An AIC is used to sample the received signal at each CR node. Finally, the determination of which bands are occupied by licensed users (LUs) at the fusion center.

2-2 Compressed Sensing of Analog Signals and the Restricted Isometric Property x(t), $t \in [0,T]$

We present an analog signal x(t), in a discrete format as a finite weighted sum of the basic elements as [7]~[9]:

$$x(t) = \sum_{i=1}^{N} s_i \psi_i(t) \tag{1}$$

where $\mathbf{x}$ is an $N \times 1$ vector $\mathbf{x} = \mathbf{\Psi s}$, which is represented in the sparse form of an $N \times 1$ vector $\mathbf{s}$ with $K << N$ non-zero elements s_i via the $N \times N$ matrix $\mathbf{\Psi}$. CS demonstrates that $\mathbf{x}$ can be recovered using $M << N$ measurements [13]. The measurements $\mathbf{y}$ are expressed as:

$$\mathbf{y} = \mathbf{\Phi x} + \mathbf{n} = \mathbf{\Phi \Psi s} + \mathbf{n} \tag{2}$$

Several choices are available for the distribution of $\mathbf{\Phi}$, such as the Gaussian, Bernoulli, or Fourier ensembles.

The reconstruction stage is performed by solving the following standard approach to an objective function as according to:

$$\min_{s} \|\mathbf{s}\|_1 \quad s.t. \quad \mathbf{y} = \mathbf{\Phi \Psi s} \tag{3}$$

The problem (3) can be efficiently solved using BP or some types of constructive algorithms such as matching pursuit (MP) and OMP [3], [4].

In order to ensure the accuracy of each reconstruction algorithm, the projected matrix $\mathbf{\Phi}$ must satisfy the RIP [14], which is presented as follows:

Definition 1 (Truncation): Let $\mathbf{\Phi} \in \mathbf{R}^{M \times N}$ $\mathbf{\Phi} \in \mathbf{R}^{M \times N}$ $\mathbf{\Phi} \in \mathbf{R}^{M \times N}$ and $\mathbf{x} \in \mathbf{R}^N$. The matrix $\mathbf{\Phi}_T$ with $T \subset \{1, \cdots, N\}$ has an *i*-th column $(i \in T)$ in $\mathbf{\Phi}$ and x_T is calculated through $\mathbf{\Phi}_T$.

Definition 2 (RIP): The matrix $\mathbf{\Phi} \in \mathbf{R}^{M \times N}$ satisfies the RIP with (K, σ_K) for $K \le M, 0 \le \sigma_K \le 1$, if

$$(1-\sigma_K)\|\mathbf{q}\|_2^2 \le \|\mathbf{\Phi}_T \mathbf{q}\|_2^2 \le (1+\sigma_K)\|\mathbf{q}\|_2^2 \tag{4}$$

for all $T \subset \{1, \cdots, N\}$ and for all $q \in \mathbf{R}^{|T|}$, and $(1-\sigma_K) \le \lambda_{\min}(\mathbf{\Phi}_T^H \mathbf{\Phi}_T) \le \lambda_{\max}(\mathbf{\Phi}_T^H \mathbf{\Phi}_T) \le (1+\sigma_K)$, where $\lambda_{\min}(\mathbf{\Phi}_T^H \mathbf{\Phi}_T)$ and $\lambda_{\max}(\mathbf{\Phi}_T^H \mathbf{\Phi}_T)$ represent the minimal and maximal eigenvalues of $\mathbf{\Phi}_T^H \mathbf{\Phi}_T$, respectively.

Ⅲ. Compressive Spectrum Sensing at a Single CR [6], [10]

In this section, we summarize the procedures for the receiving and reconstruction at each CR node.

Fig. 1 shows that the analog input $\mathbf{x}(t)$ is $\mathbf{x}_k = [x_{kN+i}]^T$, and the output of AIC is $\mathbf{y}_k = [y_{kM+j}]^T$ where $k = 0,1,2\ldots$, $i = 0,\ldots,N+1$, and $j = 0,\ldots,M+1$. The AIC is modeled by the $M \times N$ projected matrix $\mathbf{\Phi}_A$ as

$$\mathbf{y}_k = \mathbf{\Phi}_A \mathbf{x}_k \tag{5}$$

Using some mathematical operations [6], [10], we have

$$\mathbf{r}_y = \mathbf{\Phi r}_x \tag{6}$$

where $\mathbf{r}_x = [0 \quad r_x(i)]^T$ and $\mathbf{r}_y = [0 \quad r_y(i)]^T$, $i = -N+1,\ldots, N+1$ are $2N \times 1$ and $2M \times 1$ autocorrelation vectors, respectively.

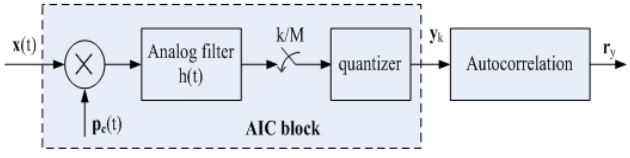

Fig. 1. CS acquisition at an individual CR sensing receiver.

After acquiring the output vector of the autocorrelation operation, we use the wavelet-based approach as presented in [15], [16] to detect the band edge locations. For an experiment when $N \ll M$ in [5], the edge spectrum $\mathbf{z}_s$ can be determination from measurements and the relation between $\mathbf{z}_s$ and $\mathbf{r}_x$ is:

$$\mathbf{r}_x = \mathbf{G}\mathbf{z}_s \tag{7}$$

where $\mathbf{z}_s$ is the discrete $2N \times 1$ vector and $\mathbf{G} = (\mathbf{\Gamma} FW)^{-1}$. The $2N \times 2N$ matrices $\mathbf{\Gamma}$, W, and F represent a first derivative operation, Wavelet, and Fourier transforms, respectively.

Combining (6) and (7), the optimization problem for an edge spectrum reconstruction is given by:

$$\min \|\mathbf{z}_s\|_1 \; s.t. \;\; \mathbf{r}_y = \mathbf{\Phi}\mathbf{G}\mathbf{z}_s \tag{8}$$

To solve this problem, we use the CWSS based SP (CWSSSP) that is presented in the next section. The spectrum estimate can now be evaluated as a cumulative sum of elements in vector $\hat{\mathbf{z}}_s = [\hat{z}_s(i)]^T$, $i = 1, \ldots, 2N$. Therefore, the estimated values of PSD are given by

$$\hat{S}_x(n) = \sum_{k=1}^{n} \hat{z}_s(k) \tag{9}$$

Ⅳ. Collaborative Compressed Spectrum Sensing

In Fig. 2, $x_j(t)$ is the input of AIC at the j-th CR node. The output of AIC is processed to give the $2M \times 1$ autocorrelation vector $\mathbf{r}_{y,j}$. The fusion center collects the autocorrelation vectors and applies the DCWSSSP approach to reconstruct the J received PSD $\hat{S}_{x,j}$; $j = 1, \ldots, J$ and then obtains an average PSD. Finally, the center determines whether the frequency ranges are occupied, based on the average PSD.

4-1 Overview of the SP Approach [17]

The SP algorithm [17] is less complicated but it results in a comparable recovery performance to LP techniques.

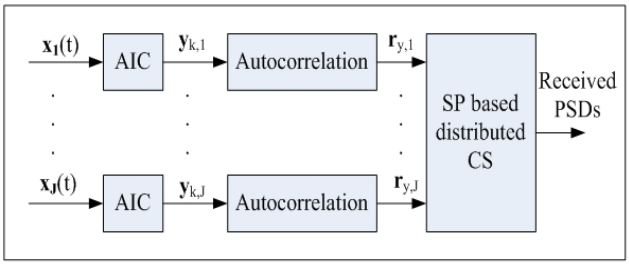

Fig. 2. DCWSS for multiple CR nodes.

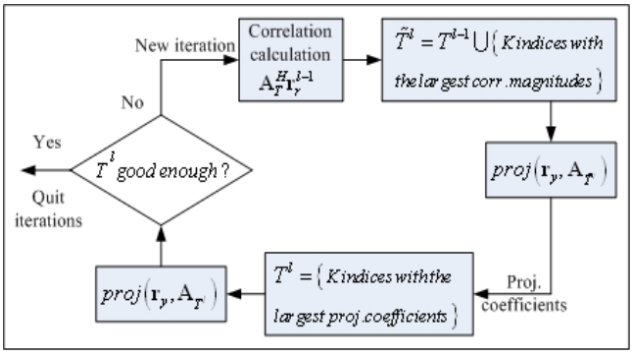

Fig. 3. Subspace pursuit algorithm applied to reconstruction.

First, the matrix $\mathbf{A} = \mathbf{\Phi}\mathbf{G}$ can be expressed in a row of its columns as:

$$\mathbf{A} = [\mathbf{a}_1 \quad \mathbf{a}_2 \quad \cdots \quad \mathbf{a}_{2N}] \tag{10}$$

The next step is solving the problem (8) by using an SP technique. We set the truncation for subspace $\mathbf{A}_S$ of the matrix $2M \times 2N$ $\mathbf{A}$ as in Definition 1, Section III and $span(\mathbf{A}_S)$ is represented to the space span of $\mathbf{A}_S$. In addition, the matrix $2M \times 2N$ $\mathbf{A}$ also satisfies the RIP, as in (4), Definition 2, Section III, by replacing M by $2M$, N by $2N$, each $\mathbf{\Phi}_T$ by $\mathbf{A}_S$, and each $\mathbf{\Phi}$ by $\mathbf{A}$.

The $l1$-linear program approach can successfully reconstruct a K-sparse signal if the RIP must be satisfied with constants σ_K, σ_{2K} and σ_{3K}, which have a condition $\sigma_K + \sigma_{2K} + \sigma_{3K} < 1$ [18]. However, in [14], the authors improved the above condition to $\sigma_{2K} < \sqrt{2} - 1$. For any given vector $\mathbf{r}_y \in \mathbf{R}^{2M}$, the projection of $\mathbf{r}_y$ onto the subspace $span(\mathbf{A}_S)$ is denoted by $\mathbf{r}_{y,p}$ and can be computed as:

$$\mathbf{r}_{y,p} = proj(\mathbf{r}_y, \mathbf{A}_S) := \mathbf{A}_S \mathbf{A}_S^{\dagger} \mathbf{r}_y \tag{11}$$

Note that $\mathbf{A}_S^{\dagger} = (\mathbf{A}_S^H \mathbf{A}_S)^{-1} \mathbf{A}_S^H$ is the pseudo-inverse of the matrix $\mathbf{A}_S$, where subscript ^{H} denotes the conjugate transposition. Corresponding to the projection vector, the projection residue vector $\mathbf{r}_{y,r}$ is defined as

$$\mathbf{r}_{y,r} = resid(\mathbf{r}_y, \mathbf{A}_S) := \mathbf{r}_y - \mathbf{r}_{y,p} \tag{12}$$

Fig. 3 illustrates the schematic diagram of iterations in the SP algorithm [17], demonstrating that the subspace is updated during each iteration; i.e., elements can be added to or deleted from the subspace.

The following subsection represents the algorithm to solve the above problem.

4-2 The Jointly Recovery SP Algorithm

The advantage of the SP algorithm comparing with the OMP method is the way to generate S^l, that is the estimate of the correct support set S.

We describe the procedure of this algorithm as follows:

1. Input:

· A $2M \times 2N$ matrix A.

· A $2M \times J$ input matrix $\mathbf{R} = \left[\mathbf{r}_{\mathrm{y},1} \;\; \mathbf{r}_{\mathrm{y},2} \;\; \cdots \;\; \mathbf{r}_{\mathrm{y},J}\right]$ received from J CR sensing receivers.

2. Output: The $2N \times J$ estimated signal $\mathbf{Z}_{\mathrm{s}} = \left[\mathbf{z}_{\mathrm{s},1}, \mathbf{z}_{\mathrm{s},2}, \cdots \mathbf{z}_{\mathrm{s},J}\right]$, the average of j PSD estimate vectors $\hat{\mathbf{S}}_{\mathrm{x}}^{(J)}$.

3. Procedure:

1) Initialization:

· For each j-th CR (j=1, …, J), we have

$$S_j^0 = \left\{ \begin{matrix} K\ indices\ with\ respect\ to\ the\ largest \\ elements\ in\ \mathbf{A}^{\mathrm{H}}\mathbf{r}_{y,j} \end{matrix} \right\} = \left[\upsilon_{j,1}^0 \;\; \upsilon_{j,2}^0 \;\; \cdots \;\; \upsilon_{j,K}^0\right]$$

and then calculate

$$S^0 = average\left\{S_j^0\right\} = \left[\upsilon_1^o \;\; \upsilon_2^0 \;\; \cdots \;\; \upsilon_K^0\right]'$$

Where $\upsilon_k^o = \frac{1}{J}\sum_{j=1}^{J}\upsilon_{k,j}^o$.

· The projection residue vector for the j-th CR is $\mathbf{r}_{r,j}^0 = resid\left(\mathbf{r}_{y,j}, \mathbf{A}_{\hat{S}^0}\right)$.

2) Iteration: The following steps will be performed at every $l-th$ iteration.

· For each j-th CR (j=1, …, J), we evaluate

$$\hat{S}_j^{l-1} = \left\{ \begin{matrix} K\ indices\ respect\ to\ the\ largest \\ elements\ in\ \mathbf{A}^{\mathrm{H}}\mathbf{r}_{r,j}^{l-1} \end{matrix} \right\},$$

$$\hat{S}_j^{l-1} = average\left\{S_j^{l-1}\right\} = \left[\upsilon_1^{l-1} \;\; \upsilon_2^{l-1} \;\; \cdots \;\; \upsilon_K^{l-1}\right] \quad (13)$$

where

$$\upsilon_k^{l-1} = \frac{1}{J}\sum_{j=1}^{J}\upsilon_{k,j}^{l-1},\ k = 1, 2, \ldots, K, \quad (14)$$

and then $\tilde{S}^l = S^{l-1} \cup \hat{S}^{l-1}$.

· For each j-th CR, we set the projection coefficients: $\mathbf{z}_{s,p,j} = \mathbf{A}_{\tilde{S}^l}^{\dagger}\mathbf{r}_{y,j}$.

· $S_j^l = \left\{ \begin{matrix} K\ indices\ with\ respect\ to\ the\ largest \\ elements\ in\ \mathbf{z}_{s,j} \end{matrix} \right\}$; And we calculate S^l using (13), (14) and replacing $(l-1)$ with l.

· The residue vector of the projection for the j-th CR is $\mathbf{r}_{r,j}^l = resid\left(\mathbf{r}_{y,j}, \mathbf{A}_{S^l}\right)$.

3) Termination test: The SP iteration is terminated when $\min\left\|\mathbf{r}_{r,j}^l\right\|_2 > \min\left\|\mathbf{r}_{r,j}^{l-1}\right\|_2$, $j = 1, 2, \ldots, J$. Then let $S^l = S^{l-1}$ and quit the iteration. If the limit is not reached, increase l and return to the iteration.

4) Store the results:

The estimated signal $\hat{\mathbf{z}}_{s,j}$ satisfies $\hat{\mathbf{z}}_{s,j}\big|_{\{1,\cdots,N\}-T^l} = \mathbf{0}$ and $\hat{\mathbf{z}}_{s,j}\big|_{S^l} = \mathbf{A}_{S^l}^{\dagger}\mathbf{r}_{y,j}$. The j-th PSD estimate vector is $\hat{\mathbf{S}}_{\mathrm{x},j}(n) = \sum_{k=1}^{n}\hat{z}_{s,j}(k)$.

The average of J PSD estimate vectors is

$$\mathbf{S}_{\mathbf{x}}^{(\mathbf{J})} = \frac{\mathbf{1}}{\mathbf{J}}\sum_{\mathbf{j}=\mathbf{1}}^{\mathbf{J}}\mathbf{S}_{\mathbf{x},\mathbf{j}}, \quad (15)$$

4-3 Performances:

4-3-1 MSE Performance

The MSE of PSD from our approach is calculated as:

$$\mathrm{MSE}^{(J)} = \mathrm{E}\left\{\frac{\left\|\hat{\mathbf{S}}_{\mathbf{x}}^{(J)} - \mathbf{S}_{\mathbf{x}}^{(J)}\right\|_2^2}{\left\|\mathbf{S}_{\mathbf{x}}^{(J)}\right\|_2^2}\right\} \quad (16)$$

where $\hat{\mathbf{S}}_{\mathbf{x}}^{(J)}$ and $\mathbf{S}_{\mathbf{x}}^{(J)}$ denote the average PSD output and the PSD, respectively for in case of signals sampled at the Nyquist rate.

4-3-2 Probability of Detection

To compute the detection probability Pd, we apply the energy detection method, where the test static is calculated from the averaged PSD estimate $\hat{\mathbf{S}}_{\mathbf{x}}^{(J)}$[19]. As in [10], we identify the static test as:

$$E_I^{(J)} = \frac{1}{JH}\sum_{i=(I-1)L+1}^{IL}\sum_{j=1}^{J}\sum_{h=1}^{H}\left|X_{h,j}(i)\right|^2 \quad (17)$$

where L is the total samples from each channel, $I = 1, 2, \ldots, maxI$, H is the total number of blocks, X represents the Fourier transform from x.

Using the Neyman-Pearson hypothesis test, we determine the decision threshold μ [19]:

$$P_f^{(J)} = 1 - \frac{\Gamma\left(JH, \frac{\mu}{JH}\right)}{\Gamma(JH)} \quad (18)$$

where $\Gamma(.,.)$ is upper incomplete gamma function [20], Sec. (8.350)], $\Gamma(.)$ is the gamma function [20], Sec. (13.10)]. Hence, the probability of detection $P_d^{(J)}$ is evaluated as

$$P_d^{(J)} = \frac{1}{a}\sum_{I=I_1}^{I_a} \Pr\left\{E_I^{(J)} > \mu\right\} \tag{19}$$

where $I_i, i = 1,\ldots,a$ denote the indices of a active channels.

Ⅴ. Simulation Results

In this section, the simulation results are shown to evaluate the proposed approach. In this simulation model, the frequency band ranges from −38.05 to 38.05 MHz, which is the same as that described in [21], and the number of channels is *maxI*=10 with 7.61 MHz bandwidth. The OFDM frame length T_F includes 68 symbols, and each of these super-frames contains four frames. The number of carriers per symbol is *C*=1,705 with a duration *TS*, composed of a useful part *TU and a guard interval* Δ (set to 0 in this simulation).

For this scheme, the over-sampling factor is 02, and only 50 % of the channels are active. The SNRs of the active channels are assumed to be in the range [−10 dB, −8 dB] and the AGWN variance is $\sigma_n^2 = 1$. The smoothing signal scheme is performed using a Gaussian wavelet. The length of input signal is 2*N*=512 and the compressed rate is varying from 5 % to 100 %, and *H*=160, and $\mathbf{\Phi}_A$ has a zero-mean Gaussian ensemble with variance 1/*M*. The number of PSD samples of each channel is *L*=25.

Fig. 4 illustrates the MSE performances for the SP, OMP, iteratively reweighted least squares with regularization (IRLS) [21] and Cosamp algorithms [22]. The results show that better performance is achieved for SP than for these other approaches, while all versions take the same time to reach convergence. The OMP algorithm has the worst performance in the conditions used for this simulation, with a low sampling factor corresponding to low sparsity and the noisy environment. The SP algorithm is robust in this case because it adds the good basis candidates and it also removes the bad candidates. This figure also shows the signal recovery quality, where MSE decreases when the compression rate *M/N* increases. However, to complement this degradation, we take advantage of the multi-CR scheme, where MSE can be significantly reduced. Therefore, we reduce the cost of high speed by using the CS method and we also improve the MSE by exploiting the multiple CRs.

Table 1. Parameters for the simulations.

Parameter	2 k mode
Elementary period T	$7/64\mu s$
Number of carriers C	1,705
Value of carrier number $C_{\min}$	0
Value of carrier number $C_{\max}$	1,704
Duration of symbol part T_U	$2,048\times T$ $224\mu s$
Carrier spacing $1/T_U$	4,464 Hz
Spacing between carriers $C_{\min}$ and $C_{\max}$ $(C-1)/T_U$	7.61 MHz

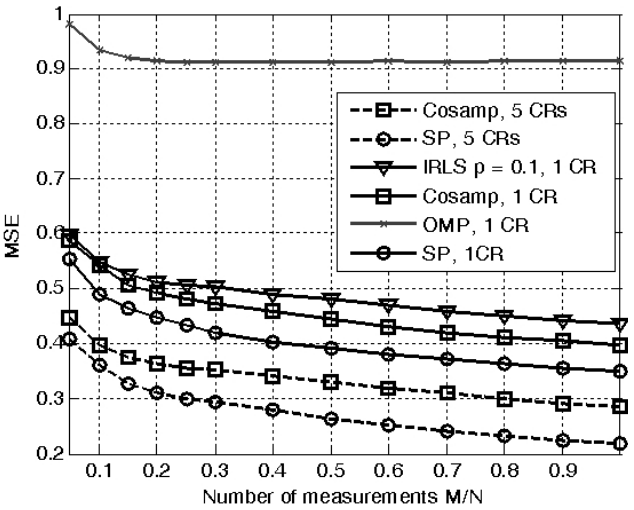

Fig. 4. MSE for SP, IRLS, OMP and Cosamp approaches versus compression rate *M/N* for various numbers of collaborating CRs (SNR=[−10 dB, −8 dB]).

The detection performance is shown in Fig. 5, which

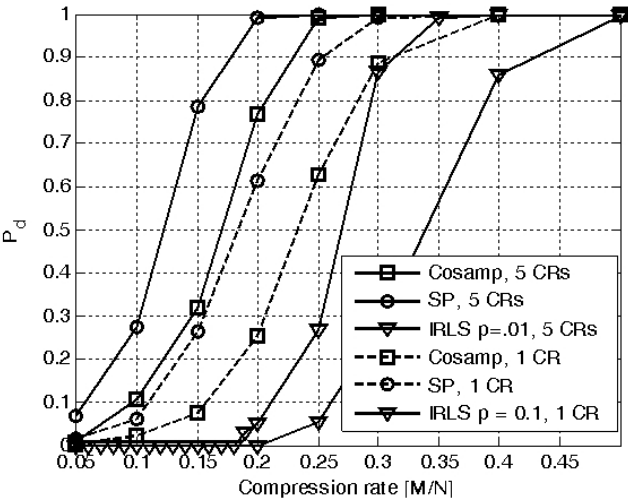

Fig. 5. Probabilities of detection P_d for SP and Cosamp approaches versus compression rate *M/N* for various numbers of collaborating CRs (SNR=[−10 dB, −8 dB]).

depicts the probability of detection $P_d^{(J)}$ vs. the compression ratio M/N when the number of CRs is J=1 and 5 at a given $P_f^{(J)}$ of 0.01. This figure demonstrates that the detection probability was high at a low compression ratio M/N. The use of multiple CRs significantly improves the detection probability. In addition, the probability of detection is improved by the SP approach compared with the IRLS and Cosamp algorithms.

Ⅵ. Conclusion

In this paper, we used the DCWSS and SP algorithm to reduce the recovery error in the reconstruction stage in the CRN. A new iterative algorithm, termed the DCW-SSSP approach, is exploited for joint compressive spectrum sensing.

This research was supported by Basic Science Research Program through the National Research Foundation of Korea(NRF) funded by the Ministry of Education, Science and Technology(No. 2010-0004-865)

References

[1] "Proc. 1st IEEE Int'l. Symp. New frontiers in dynamic spectrum access networks," Nov. 2005.

[2] http://www.ieee802.org/22/.

[3] J. A. Tropp, A. C. Gilbert, "Signal recovery from random measurements via orthogonal matching pursuit," *IEEE Transactions on Information Theory*, vol. 53, pp. 4655-4666, 2007.

[4] D. L. Donoho, "Compressed sensing," *IEEE Transactions on Information Theory*, vol. 52, pp. 1289-1306, 2006.

[5] T. Zhi, G. B. Giannakis, "Compressed sensing for wideband cognitive radios," in *IEEE International Conference on Acoustics, Speech and Signal Processing (ICASSP)*, pp. IV-1357-IV-1360, 2007.

[6] Y. L. Polo, *et al.*, "Compressive wide-band spectrum sensing," in *IEEE International Conference on Acoustics, Speech and Signal Processing (ICASSP)*, pp. 2337-2340, 2009.

[7] S. Kirolos, *et al.*, "Practical issues in implementing analog-to-information converters," in *The 6th International Workshop on System-on-Chip for Real-Time Applications*, pp. 141-146, 2006.

[8] S. Kirolos, *et al.*, "Analog-to-information conversion via random demodulation," in *IEEE Dallas Circuits and Systems Workshop (DCAS)*, Dallas, Texas, 2006.

[9] J. N. Laska, *et al.*, "Theory and implementation of an analog-to-information converter using random demodulation," in *IEEE International Symposium on Circuits and Systems (ISCAS)*, pp. 1959-1962, 2007.

[10] W. Ying, *et al.*, "Distributed compressive wide-band spectrum sensing," in *Information Theory and Applications Workshop*, pp. 178-183, 2009.

[11] M. F. Duarte, *et al.*, "Distributed compressed sensing of jointly sparse signals," in *Conference Record of the Thirty-Ninth Asilomar Conference on Signals, Systems and Computers*, pp. 1537-1541, 2005.

[12] D. Needell, J. A. Tropp, "CoSaMP: Iterative signal recovery from incomplete and inaccurate samples," *Applied and Computational Harmonic Analysis*, vol. 26, pp. 301-321, 2008.

[13] E. C. a. J. Romberg, "Sparsity and incoherence in compressive sampling," *Inverse Problems*, vol. 23, no, 3, pp. 969-985, Jun. 2007.

[14] E. J. Candès, "The restricted isometry property and its implications for compressed sensing," *Compte Rendus de l'Academie des Sciences*, vol. serie I, pp. 589-592, 2008.

[15] Z. Tian, G. B. Giannakis, "A wavelet approach to wideband spectrum sensing for cognitive radios," in *1st International Conference on Cognitive Radio Oriented Wireless Networks and Communications*, pp. 1-5, 2006.

[16] S. Mallat, W. L. Hwang, "Singularity detection and processing with wavelets," *Information Theory, IEEE Transactions on*, vol. 38, pp. 617-643, 1992.

[17] D. Wei, O. Milenkovic, "Subspace pursuit for compressive sensing signal reconstruction," *IEEE Transactions on Information Theory*, vol. 55, pp. 2230-2249, 2009.

[18] E. J. Candes, T. Tao, "Decoding by linear programming," *IEEE Transactions on Information Theory*, vol. 51, pp. 4203-4215, 2005.

[19] H. L. Van Trees, *Detection, Estimation, and Modulation Theory. Part 1, Detection, Estimation, and Linear Modulation Theory*, New York: Wiley, 2001.

[20] I. S. Gradshteyn, *et al.*, *Table of Integrals, Series and Products*, 7th Ed. Amsterdam ; Boston: Elsevier, 2007.

[21] R. Chartrand, Y. Wotao, "Iteratively reweighted algorithms for compressive sensing," in *IEEE International Conference on Acoustics, Speech and Signal Processing (ICASSP)*, pp. 3869-3872, 2008.

[22] D. Needell, *et al.*, "Greedy signal recovery review," in *Signals, Systems and Computers, 2008 42nd Asilomar Conference on*, pp. 1048-1050, 2008.

Le Thanh Tan

received the B.S. degrees in Telecommunication Engineering from Poly-technique University of Danang, Vietnam in 2005. In 2008, he got the degree of Master from Hochiminh University of Technology, Vietnam in major of Electrical and Electronics Engineering. Since 2010, he has been studying Ph.D. program at University of Ulsan, Korea. His major researches are Cognitive Radio Network, Cooperative Communication.

Hyung-Yun Kong

received the M.E. and Ph.D. degrees in electrical engineering from Polytechnic University, Brooklyn, New York, USA, in 1991 and 1996, respectively, He received a B.E. in electrical engineering from New York Institute of Technology, New York, in 1989. Since 1996, he has been with LG electronics Co., Ltd., in the multimedia research lab developing PCS mobile phone systems, and from 1997 the LG chairman's office planning future satellite communication systems. Currently he is a professor in electrical engineering at the University of Ulsan, Korea. His research area includes channel coding, detection and estimation, cooperative communications, cognitive radio and sensor networks. He is a member of IEEK, KICS, KIPS, IEEE, and IEICE.